

Enhancement of a Darrius Wind Turbine by Convergent Ducting System and Study the Effect of design Parameter

Ali Abdyasser Kadhum

Assistant Lecture, Al-Furat Al-Alawsat Technical University, Kufa, Iraq; kin.ali1@atu.edu.iq

Abstract

Objectives: This study is to suggest a wind power plant in urban areas where wind speed is low. **Methods/Statistical Analysis:** The wind turbine analysis and simulation using mathematical models built in MATLAB and numerically by ANSYS FLUENT 17.2 were utilization to study the air flow performance through the duct. **Findings:** The results for approaches give a good agreement. Angles, one of the principal geometric parameters that significantly affect the convergent performances a four dimensional contraction convergent duct with the same length (1 meter) but different input areas is considered. Numerical simulations and analyses results show that the ratio between velocities recorded in the inlet section and the free stream velocity increases with the increase open angle of the duct system. The power coefficient improved for the convergent duct with opening angle of 40° by 28.571%. Also from VAWT analysis, the influence of design parameters on the power factor was achieved. Blades number effect shows that when the blade number increases the power coefficient is high too, and it is noticed that the power coefficient is increased with the rotor radius. **Application/Improvements:** Ducted system utilization for increase the productivity of wind turbines with different configurations are facing the restriction of low wind speed and improved wind turbine output capacity.

Keywords: Convergent Ducting, Design Parameter

1. Introduction

The Development in technologies of renewable energy have been become one of the most important role due to the global warming because the high consumption of energy and the fossil fuel waste it's effected on the environment this lead to deal with these alternative fuels to get energy.

At recent years the wind energy has developed into one of the highest developing sources of renewable energy¹. Many researches tried to enhance the performance of wind turbines by adding a duct to the turbine the ducting system used to provide the desired wind velocity faced the turbine² as a study in 2013 claimed that the Venturi effect was used to focus airflow to turbine blades. Wind speed increases in convergent suction and the low pressure region created behind the blades by the diffuser suction. While turbines were installed in the throat section to study the behavior of air flow through Venturi, ANSYS FLUENT was used and the results were compared with

the bare horizontal axis wind turbines. In³ studied the semi-empirical ducted wind turbine model. The methodology is predicated on certain assumptions and simplifications of the law conservation to compute the maximum power coefficient. This study shows that the increase in power coefficient is directly proportional to the mass flow rate. The rise of mass can only be achieved through two basic principles: reducing negative back pressure at exit and increasing area ratio⁴. In⁵ developed mathematical model for duct wind turbine and showed the turbine integrations according to a various domain of building simulation also in⁶ analyzed the performance of ducted wind turbine system and showed that the power coefficient enhancement because the increasing the mass flow rate due to increase the open angle of diffuser duct. Reduction in exit pressure after the exiting of a ducted axis wind turbine may have a gainful influence on the power coefficient. Many research attempts to study the effect of using duct structure with vertical axis wind turbine. These studies examine the effects of increased energy using wind

tunnel experiments⁷⁻⁹. The convergent duct system is considered in this study. Convergent airway has the ability to accelerate airflow through the convergent and increase the energy that can be drawn from the airflow.

2. Methodology of Analysis and Design of the Convergent Ducting System

The flow is considered steady, one dimensional and incompressible. The domain in convergent duct is divided into a series segment Δx thus¹⁰:

$$\Delta x = L / N - 1 \tag{1}$$

Area at each section may be calculated as:

$$A_i = A_1 - 2(A_{in} - A_n) (x_i/L) + (A_1 - A_n)(x_i^2/L^2) \tag{2}$$

Where $x_i = x_{i-1} + \Delta x$. The density is constant as the flow is incompressible so the velocity at both sections can be calculated from:

$$V_i = V_{in} A_{in} / A_i \tag{3}$$

The pressure found using a first order finite difference approximation up-wind differencing method as follows

$$P_i = P_{i-1} - \rho_i V_i (V_i - V_{i-1}) \tag{4}$$

3. The Analysis of Vertical Axis Wind Rotor

When analysis the performance for wind turbine of Darrius vertical axis, assume that there is no difference in velocity of the straight vertical blade, so it is subjected to the same flow rate along its length. Figure 1 show the velocities and flow blade angles. According to^{11,12} the velocity induces reduced in the horizontal flow tube direction, thus the induced velocity at an upstream part for rotor as:

$$= a_u \tag{5}$$

Since the upstream velocity is a lesser amount of free flow velocity, so a_u is less than 1. The downstream velocity at the downstream as:

$$= (2 - a_u) a_d \tag{6}$$

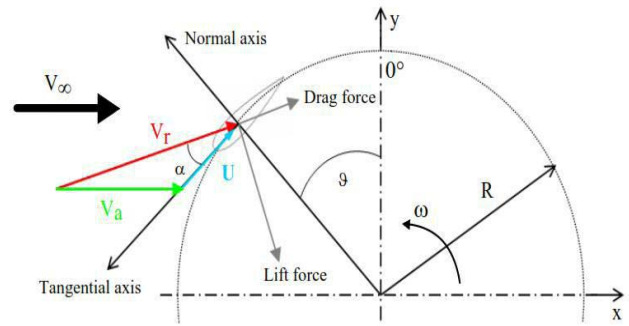


Figure 1. Velocities and flow blade angles¹¹.

Interference factor at downstream is less important of the upstream part. The local tip speed ratio (λ) can be calculated from:

$$\lambda_u = \omega R / U_t \tag{7}$$

The formula for calculating the attack angle of blade as:

$$\alpha = \arcsin \left(\frac{\lambda \sin \theta}{\lambda \sin \theta + \cos \theta} \right) \tag{8}$$

$$\lambda \sin \theta + \cos \theta$$

The normal and tangential force coefficients may be determined by,

$$C_n = C_l \cos \alpha + C_d \sin \alpha \tag{9}$$

$$C_t = C_l \sin \alpha - C_d \cos \alpha \tag{10}$$

The up-wind flow conditions are specified by:

$$F = B \int_{-0.5\pi}^{0.5\pi} \sec \theta * C_n * \cos \theta - C_t * \sin \theta d\theta \tag{11}$$

$$8 * \pi * R \tag{12}$$

up

The upstream induction factor is: a_u

The torque produced can be computed as follows:

$$T(\theta) = 0.5 * \rho * U_t^3 * C_t * R \tag{13}$$

u

The average of upstream torque is calculated from averaging the contribution of torque of both stream tube:

$$= B \int_{-0.5\pi}^{0.5\pi} T(\theta) d\theta \tag{14}$$

$$2 * \pi * 0.5\pi$$

The average torque coefficient C_t is then calculated from:

$$= T_{av} \quad (15)$$

$$0.5 * \rho * V_0^2 * A * R$$

Finally, the power coefficient C_{p_u} of the upstream half may be calculate from:

$$= * \lambda_u \quad (16)$$

Also, power coefficient (C_d) and average torque (T_d) in downstream of the vertical axis wind turbine are obtained. The overall power coefficient for the vertical axis in rotor of wind turbine rotor is a summation of the up and down power coefficients as:

$$= C_{p_u} + C_{p_d} \quad (17)$$

4. Numerical Analysis of the Duct Wind Turbine

The flow inside the duct and over the VAWT blade is solved numerically using ANSYS-FLUENT 2017. Wind turbine blades were designed with a symmetrical airfoil NACA 0012. A 2D analysis for this airfoil is treated using analysis. The convergent duct system for different geometry formed after creates the geometry of airfoil. Three airfoils are created for blading and separated by angle of 120°. Solutions by using the numerical methods demand accurate meshing for the geometry. The quality for the mesh affected by accuracy for the solution of the numerical the precision of numerical solution depending on the mesh size. The smaller mesh size needed to produce more accuracy result Table 1 shows meshing characteristics.

Table 1. Meshing characteristics

Statistics	
Nodes	215895
Elements	211237
Mesh Metric	Skewness
Min	5.8341e-005
Max	0.72573
Average	0.13289
Standard Deviation	0.10881

The performance inlet conditions and the design choices of the present study were set basing on experience.

Boundary condition and reference values of convergent duct wind turbine review in Tables (2 and 3). The results are getting from computations by CFD and it is a grid independent.

Table 2. Boundary conduction

Viscous Model	
Model	K-w
K-omega	SST
Model constants	Default
Inlet boundary condition	
Type	Inlet velocity
Velocity magnitude(m/s)	10
Reference Frame	Absolute
Turbulent method specification	Ratio of intensity and viscosity
Outlet boundary condition	
Type	Pressure outlet
Gage pressure (Pa)	101325
Back flow direction specification method	Normal to Boundary
Turbulent specification method	Magnitude normal to boundary

Table 3. Reference values

Chord Length	0.2m
Radius of the rotor	0.5m
Pressure	101325 pa at inlet velocity
Density	1 kg/m ³
Temperature	288 K

The principle is that the results mustn't vary with the number of cells inside the mesh, grid independence is consider as a one of the critical variables as taken in order to inspect the accuracy that appeared in the solution. Mesh quality such as low orthogonal quality or high skewness value are not preferred generally to keep minimum orthogonal quality > 0.1, or maximum skewness < 0.95. However, these values may defer depending on physical consideration.

The average torque depends on moment coefficient is used in FLUENT to complete the cycle. The average torque is gotten by the equation¹³.

$$C_m = C_{m1} + C_{m2} + C_{m3} \quad (18)$$

$$T_{mean} = 0.5 C_m \rho AV^3 R \text{ number of values recorded} \quad (19)$$

Where C_{m1}, C_{m2}, C_{m3} are the moment coefficients for three airfoils sequentially. The power coefficient can be determined by:

$$C P = w * T 0.5\rho AV^3 \quad (20)$$

5. Result and Discussion

The performance of the VAWT was noticed to be higher depending on λ . At high λ , the maximum angle attack value of the attained is low. Thus on the higher stream element the angle attack decreases with increase λ . While in the downstream, this variation is reversed because of the tendency of the blade relative to the wind direction shown in Figure 2. Angles of attack determines the drag and lift coefficients. High lift/drag ratio means high performance of the VAWT attained from minimum drag with higher lift Figure 3 illustrated the difference of coefficient drag and lift with attack angle changes from 35° to -35 . It is establish that's attack angle of 10° is an optimum. The power coefficient increased swept area of rotor Figure 4 shows the change in the power coefficient at different rotor radii. It is mean the power coefficient increase with rotor radius. Figure 5 illustrated the increase of power coefficient with number of blades and reduces the impact of wind magnitude and direction. The wind turbine performance is dependable of increase in the speed of the air because of the cubic dependency on it. Also the duct leads to increasing the wind speed due to the reduction area, with the law of continuity for designed convergent duct to attain the desired wind velocity at face turbine. The convergent angles of duct is from 10° to 40° causing an increment in wind velocity at inlet suction with increase inlet duct angle as shown in Figure 6.

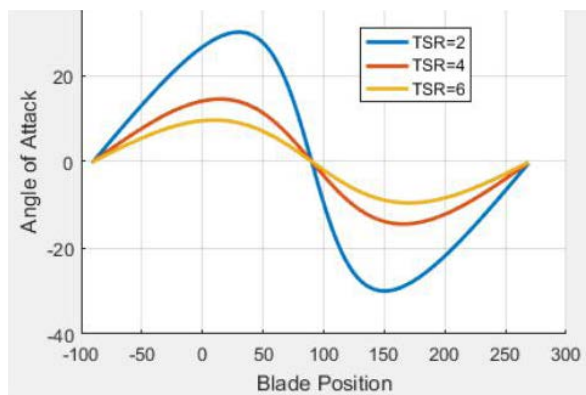


Figure 2. Blade position with angle attack.

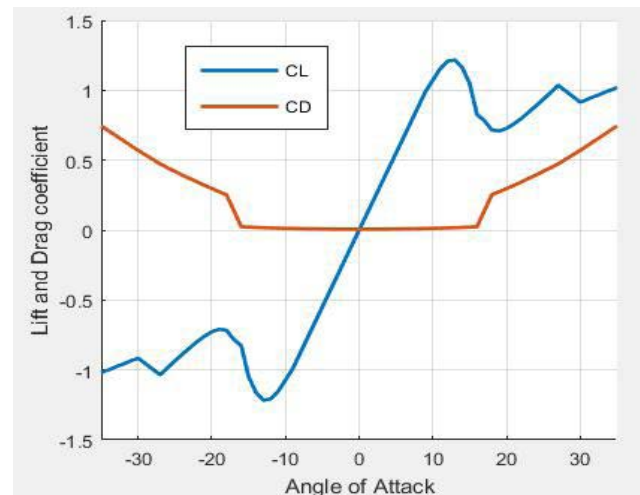


Figure 3. Drag and lift coefficient changing with angle attack.

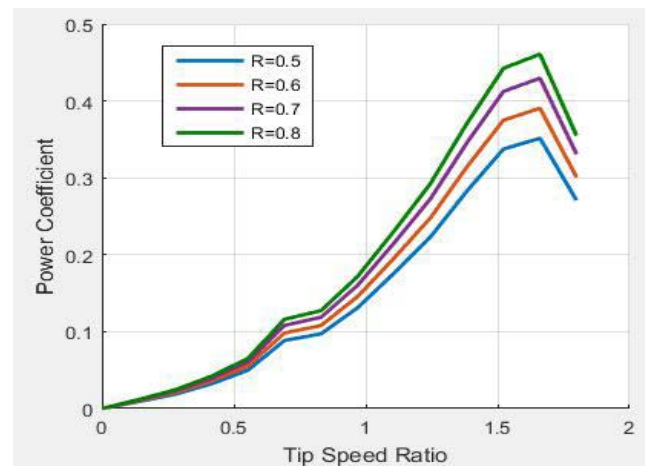


Figure 4. Effect rotor radius on power coefficient.

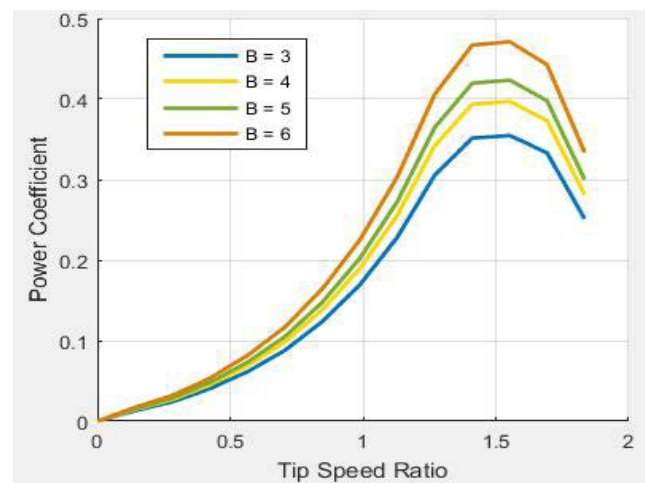


Figure 5. Blade number (B) influence on the power coefficient.

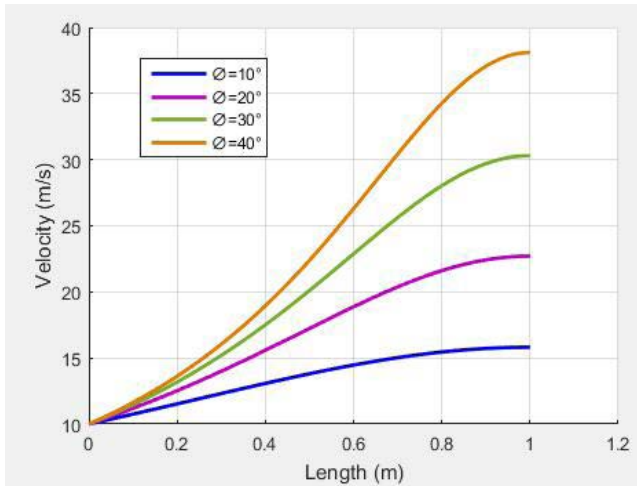


Figure 6. Velocity distribution along the converging duct.

The decrease in pressure is considered a loss of energy, but from the distribution of pressure through the duct we conclude that the decrease in pressure is very little compared with the increase in speed shown in Figure 7.

Figures 8-11 show that, in all cases of convergent duct the wind speed increases with decreasing the segment area of the duct, and it reaches a maximum value at the wind turbine inlet. Therefore the convergent duct

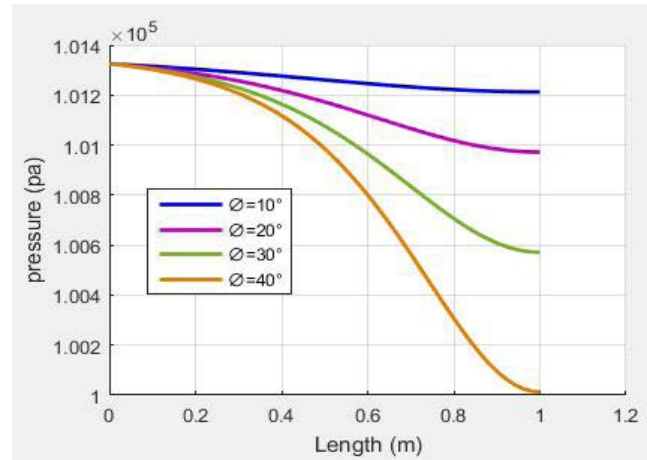


Figure 7. Pressure drop along the convergent duct.

system is a good idea used to increase the power coefficient. Vertical axis of wind turbine kind with the adaptive ducting system is modeled, simulated and valued numerically. Figure 12 and 13 show velocity variation and the corresponding changing in pressure contour for the non-ducted wind rotor is presented. The velocity contours show that velocity in the inlet duct equal 10 m/s, it increases gradually until the turbine entry as shown in Figure 14. This speed increase with rotation speed of

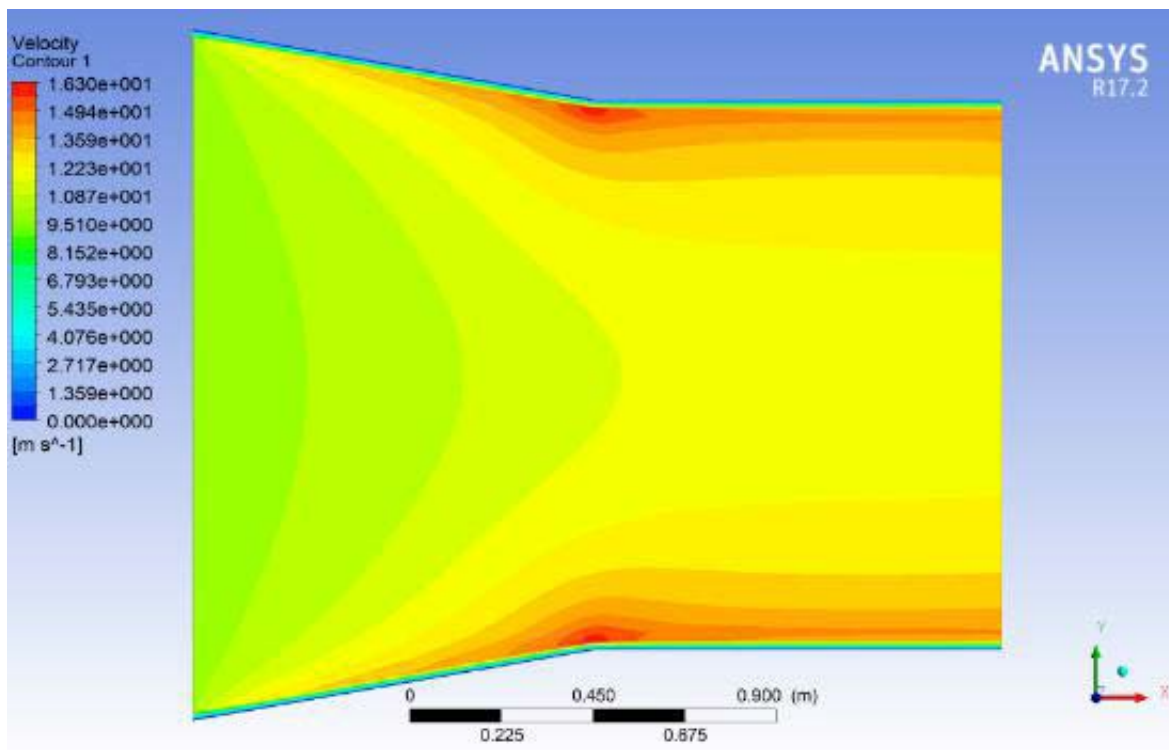


Figure 9. Flow velocity in the convergent model of inlet angle 20°.

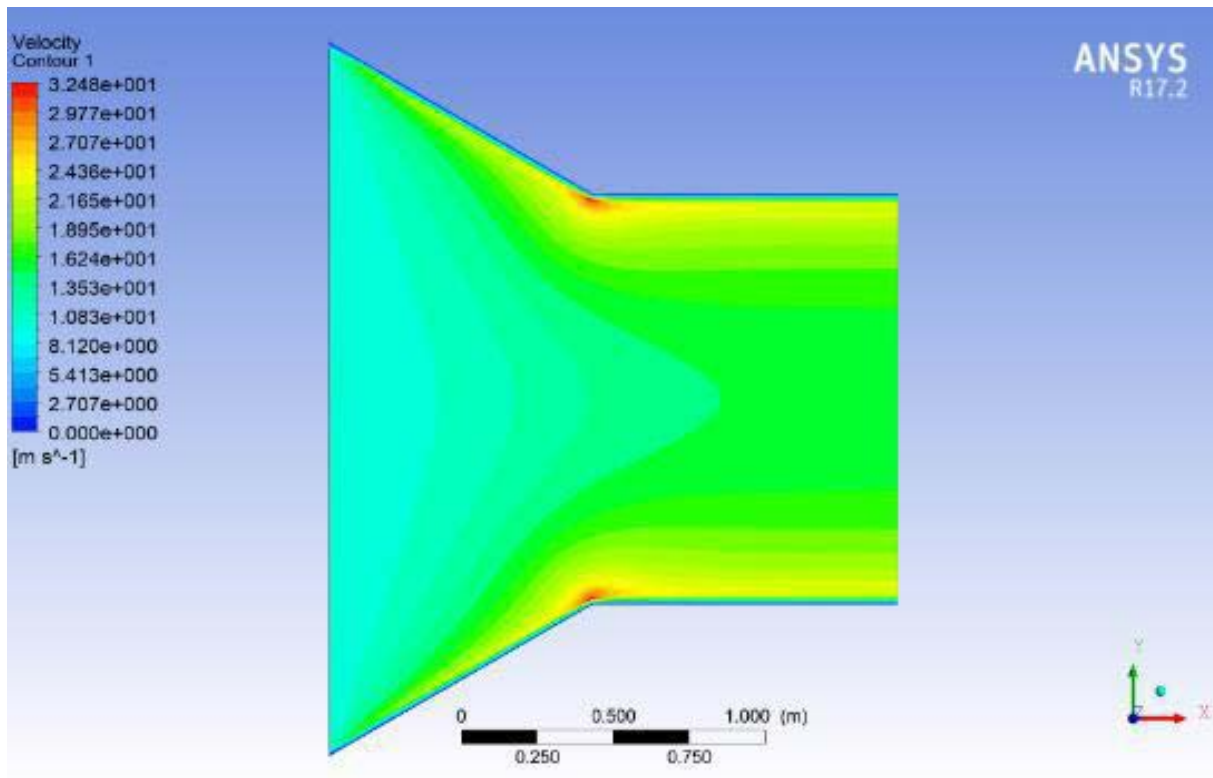


Figure 10. Flow velocity in the convergent model of inlet angle 30°.

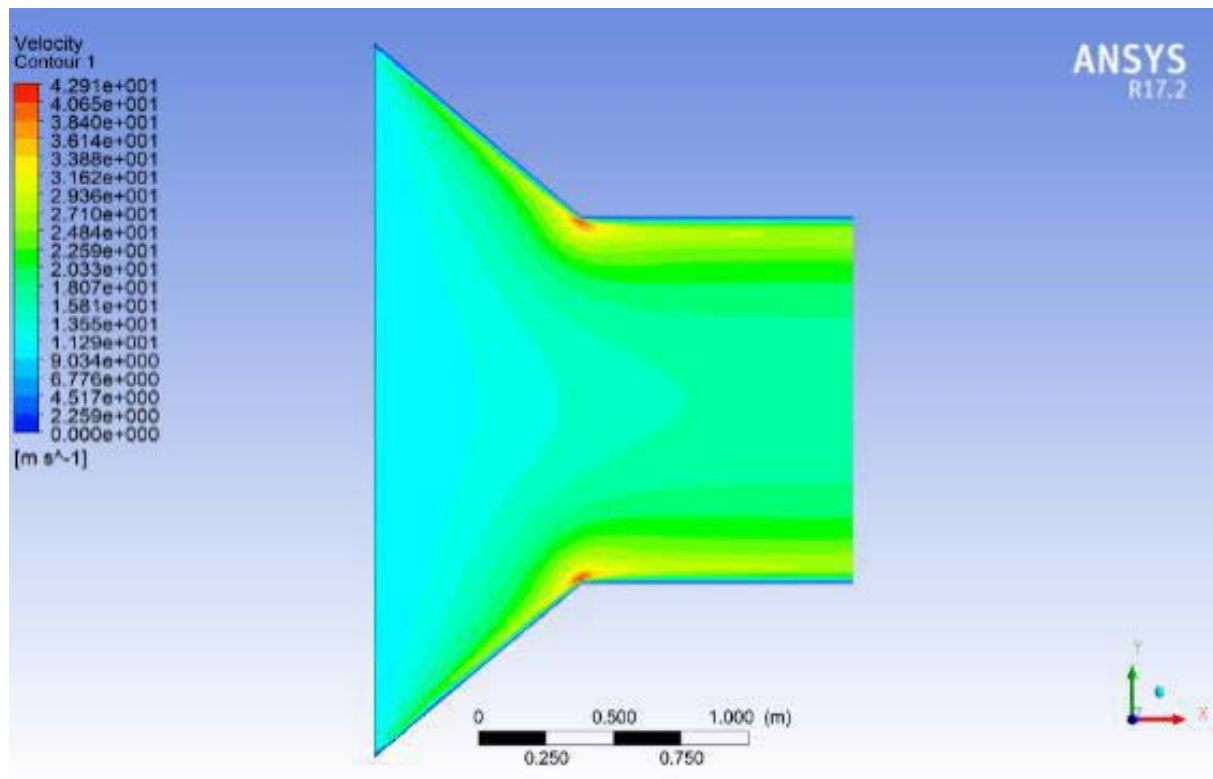


Figure 11. Flow velocity in the convergent model of inlet angle 40°.

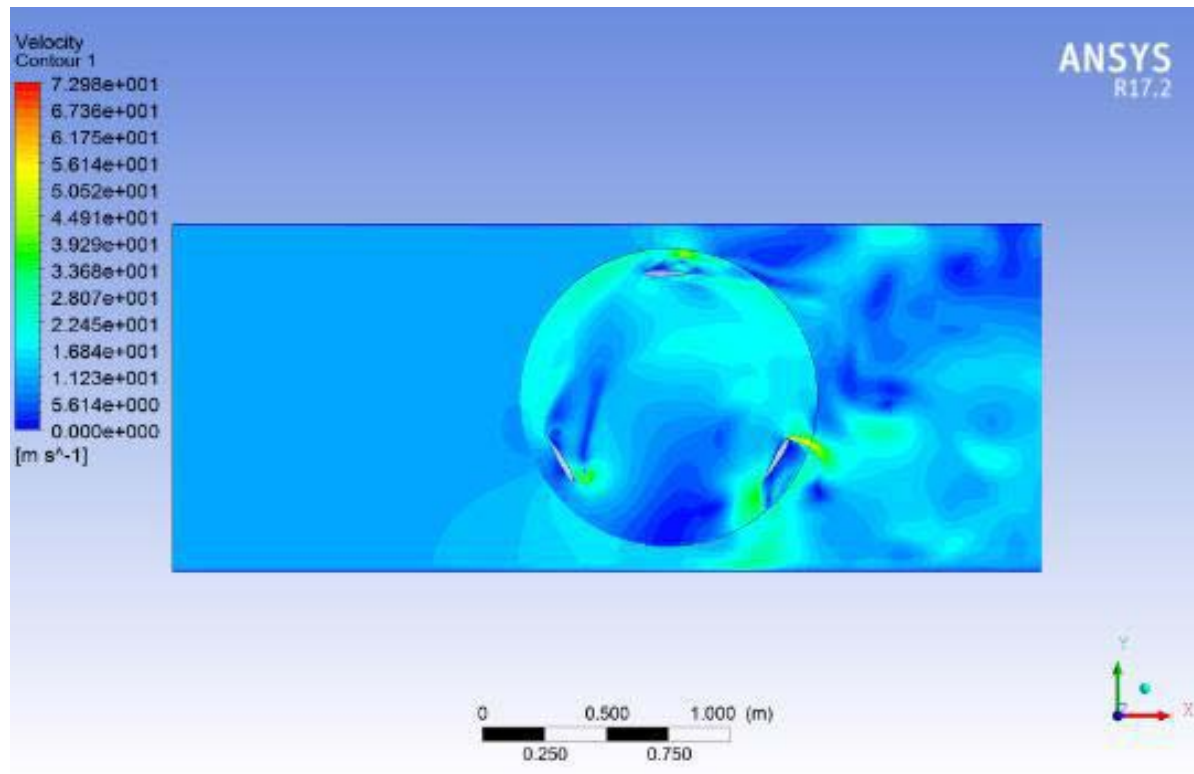


Figure 12. Velocity distribution in the non-ducted vertical axis wind turbine.

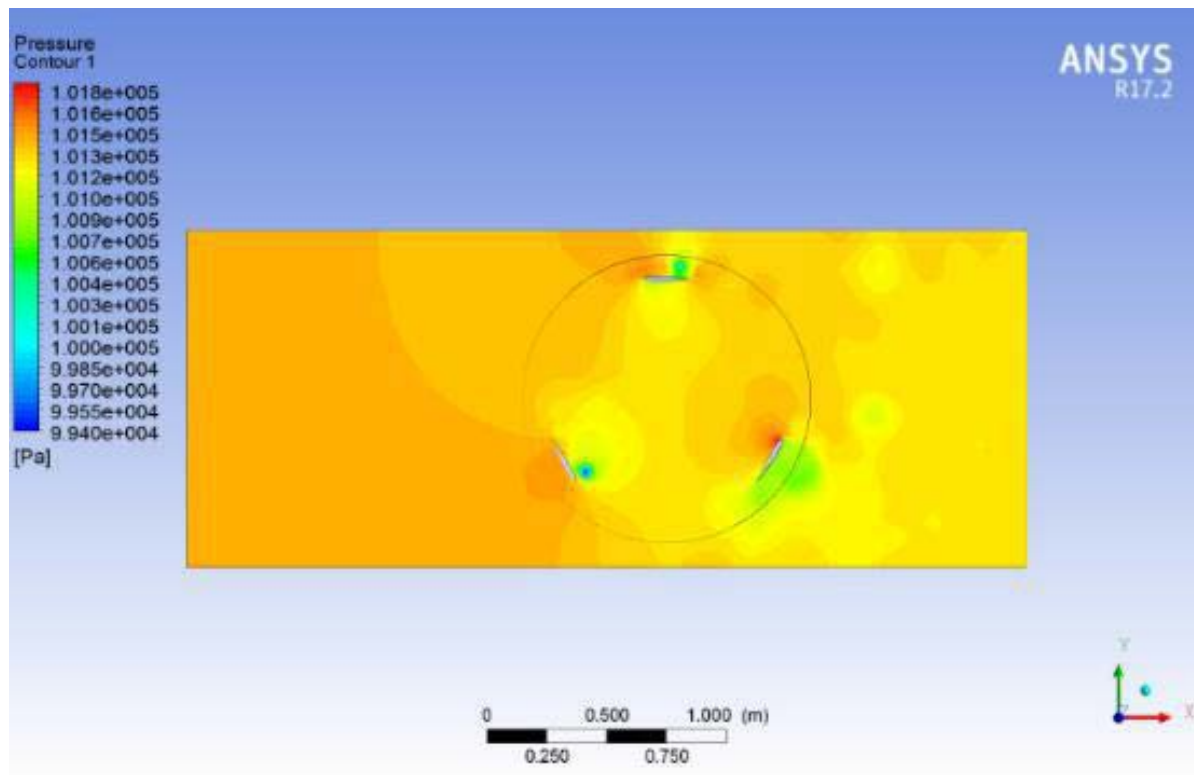


Figure 13. Variation of pressure in non-ducted vertical axis wind turbine.

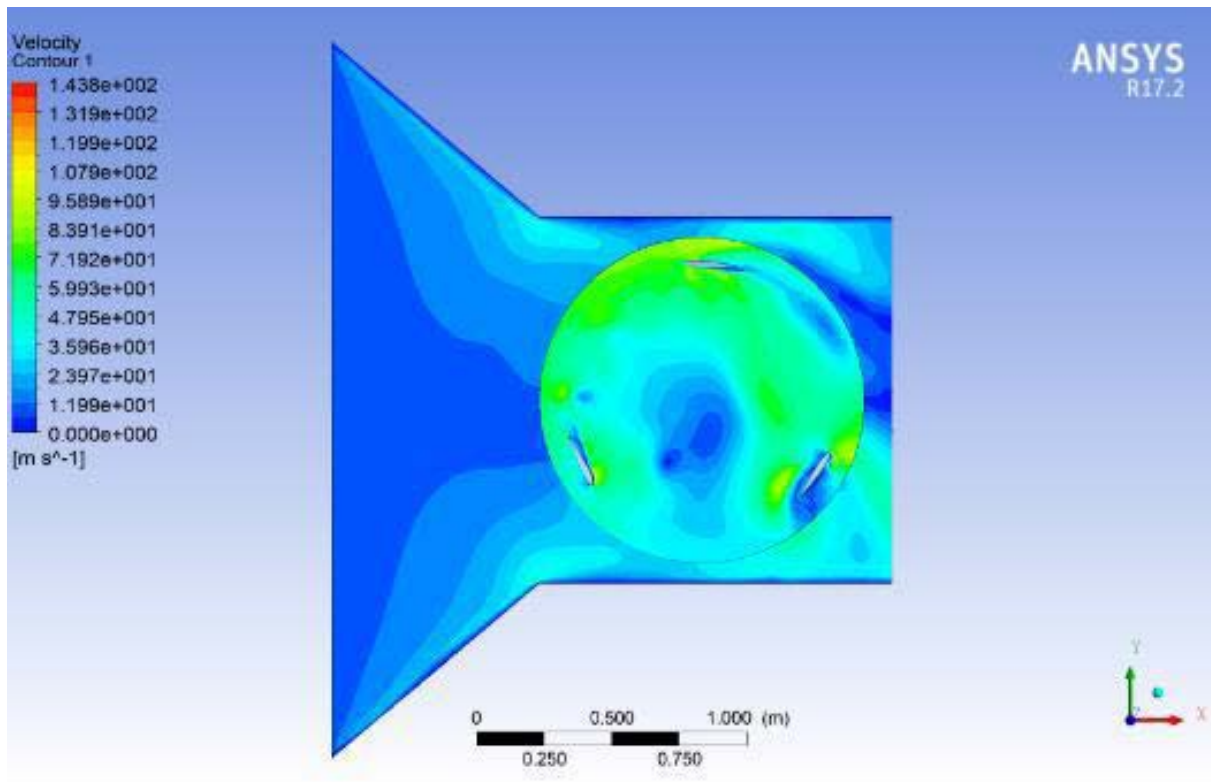


Figure 14. Flow velocity in the convergent model of inlet angle 40°.

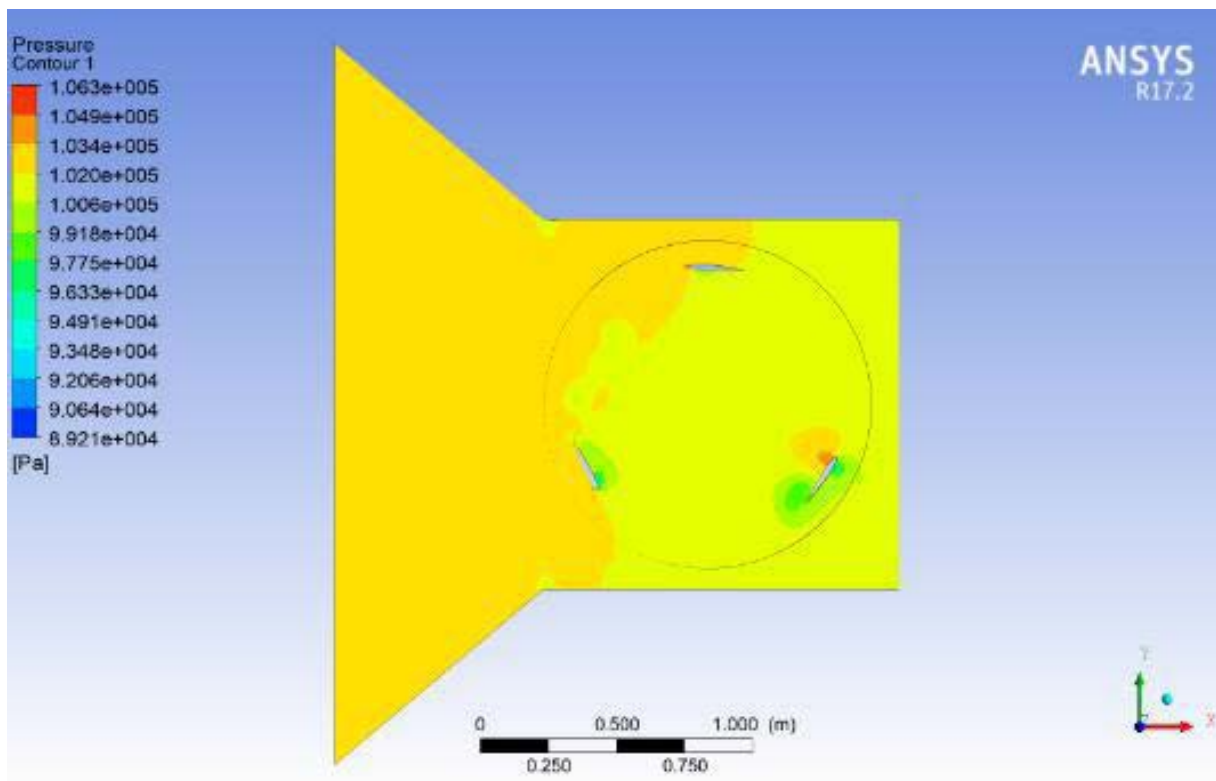


Figure 15. Pressure contour across the convergent duct of inlet angle of 40.

the turbine Figure 15 shows the pressure in the duct is gradually decreased toward the throttle. Figure 16 shows CP curves against TSR while the angle is open of the convergent duct (ϕ) are change at ($10^\circ - 40^\circ$). The results obtained that the higher ϕ generates higher output power coefficient over a wider range of TSR. Figures 17 and 18 show the variation of power coefficients of tip speed ratio of non-ducted and ducted wind turbine this show a little difference in the power coefficient value between analytical and numerical solution.

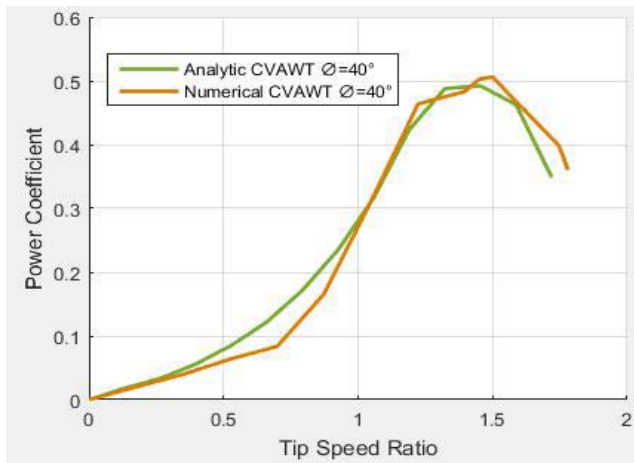


Figure 16. Power coefficient with TSR.

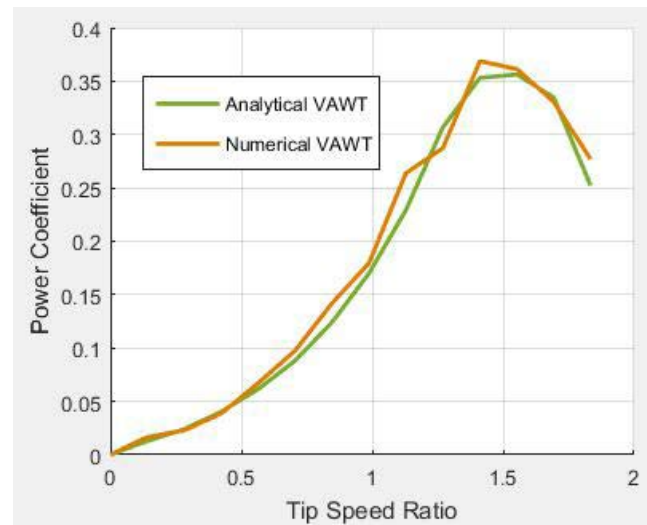


Figure 17. Power coefficient with TSR.

6. Conclusions

Developments of this study are carried out to increase the wind power productivity. In this paper, a convergent duct with different converging angles is considered. It was concluded that, increasing the angle of convergence lead to enhance the productivity and efficiency of wind turbine

Notation			
Symbol	Description	V	Velocity
A	Area	x	Local Duct length
a	Interference factor	Greek symbols	
B	Blades number	α	Angle of attack
C	Force coefficients	θ	Azimuth angle
c	Chord	ϕ	Duct angle
CL	Lift Coefficient	ρ	Air density
CD	Drag Coefficient	σ	Turbine solidity
Cp	Power coefficient	ω	The angular velocity
Cm	Torque coefficient	Abbreviations	
F	Force	CFD	Computational Fluid Dynamics
P	Power	CVAWT	Convergent vertical axis wind turbine
p	Pressure	DAWT	Ducted axis wind turbine
P_{wind}	Available wind	\bar{a}_v	Average
r	Local radius	d	Down stream
Re	Reynolds number	n	Normal
T	Torque	t	Tangential
TSR	Tip speed ratio	u	Up stream

Figure 18. Power coefficient with TSR.

for the reason that of the dependency of power on the cubic wind speed Ducting system guide to power augmentation. The power coefficient enhanced for the convergent duct with opening angle of 40° by 28.571%. This privilege assist installing wind turbine system in converging gates of buildings and in manufactured adapted ducts and consequently alleviating the use of ducted axis wind turbine systems in low wind speed regimes like Iraq. Also from VAWT analysis, the influence of design parameters on the power factor was achieved. Blades number effect shows that when the blade number increases with power coefficient, and it is noticed that the power coefficient is increased with rotor radius.

7. References

1. Thangavelu SK, Mutasher SA, Kenny Lau YH. Design and flow velocity simulation of diffuser augmented wind turbine using CFD, *Journal of Engineering Science and Technology*. 2013; 8(4):372–84.
2. Kishore RA, Coudron T, Priya S. Small-scale wind energy portable turbine (Swept), *Journal of Wind Engineering and Industrial Aerodynamics*. 2013; 116:21–31. <https://doi.org/10.1016/j.jweia.2013.01.010>.
3. Numerical Analysis of Venturi Ducted Horizontal Axis Wind Turbine for Efficient Power Generation. Date accessed: 2013. <http://www.ijmca.org/index.php/ojs/article/view/37>.
4. Optimization of Wind Duct Geometry for Maximizing Power Generation of Ducted Vertical Turbines. Date accessed: 2014. https://www.researchgate.net/publication/280927494_Optimization_of_Wind_Duct_Geometry_for_Maximizing_Power_Generation_of_Ducted_Vertical_Turbines.
5. Grant A, Kelly N. The Development of a Ducted Wind Turbine Simulation Model. Eighth International IBPSA Conference; 2003. p. 407–14.
6. The Science of Making More Torque from Wind Diffuser Experiments and Theory Revisited. Date accessed: 2007. <http://iopscience.iop.org/article/10.1088/1742-6596/75/1/012010/pdf>.
7. Watanabe K, Ohya Y, Karasudani T, Watanabe K. Application of collection-acceleration device of wind to VAWT, *Proceedings of Japan Wind Energy Symposium*. 2004; 26:147–50.
8. Takahashi S, Ohya Y, Karasudani T, Watanabe K. Numerical and Experimental Studies of Airfoils Suitable for Vertical Axis Wind Turbines and an Application of Wind-Energy Collecting Structure for Higher Performance. In: *Proceedings of the Fourth International Symposium on Computational Wind Engineering*; 2006. p. 327–30.
9. Watanabe K, Ohya Y, Karasudani T. Development of a High-Performance Vertical Axis Wind Turbine by A Drive. In: *Proceedings of the National Symposium on Wind Engineering*; 2010. p. 239–44.
10. Introduction to Compressible Fluid Flow. Date accessed: 22/07/2013. <https://www.crcpress.com/Introduction-to-Compressible-Fluid-Flow/Oosthuizen-Carscallen/p/book/9781439877913>.
11. Alaimo A, Esposito A, Messineo A, Lando C, Tumino D. 3D CFD Analysis of a vertical axis wind turbine, *Energies*. 2015; 8(4):3013–33. <https://doi.org/10.3390/en8043013>.
12. Chan TF, Lai LL. Permanent-Magnet Machines for Distributed Generation: A Review. *IEEE Power Engineering Annual Meeting*; 2007. p. 1–6. <https://doi.org/10.1109/PES.2007.385575>.
13. Vaishnav E. An Investigation on the Aerodynamic Performance of a Vertical Axis Wind Turbine. Bachelor of Science in Mechanical Engineering Bhilai Institute of Technology Durg, India; 2007. p. 1–90.